Journal of Molecular Liquids 325 (2021) 115153

Contents lists available at ScienceDirect

Journal of Molecular Liquids

journal homepage: www.elsevier.com/locate/molliq

Laser diagnostics of reverse microemulsions: Influence of the size and shape of reverse micelles on the Raman spectrum on the example of water/AOT/cyclohexane system

Ivan V. Plastinin [a,*], Sergey A. Burikov [a,b], Tatiana A. Dolenko [a,b]

[a] Skobeltsyn Institute of Nuclear Physics, Lomonosov Moscow State University, 119991, Leninsky Gory 1 Bldg. 2, Moscow, Russia
[b] Faculty of Physics, Lomonosov Moscow State University, 119991, Leninsky Gory 1 Bldg. 2, Moscow, Russia

ARTICLE INFO

Article history:
Received 3 November 2020
Received in revised form 17 December 2020
Accepted 20 December 2020
Available online 30 December 2020

Keywords:
Self-organization
Microemulsions
Reverse micelle
Surfactant
Nanotechnology
Raman scattering

ABSTRACT

In this study, the influence of the size and shape of reverse micelles in water/AOT-Na/cyclohexane microemulsions on the spectral characteristics of vibrational spectra was studied using Raman laser spectroscopy and method of dynamic light scattering. The sensitivity of the spectral bands of stretching vibrations of OH groups of water molecules and SO_3 groups of AOT anions to the processes of self-organization of surfactants in microemulsions was established and explained. It is proposed to use this sensitivity of the OH and SO spectral bands of the Raman spectrum of microemulsions to create a method of determining the size of reverse micelles using Raman spectra. For this purpose, calibration curves of the spectral characteristics of these bands on the size of the reverse micelles were obtained. It was shown that the developed method can provide the best accuracy of determining the size of spherical reverse micelles 4.4%. The proposed method of laser diagnostics of microemulsions can also be applied to microemulsions with another composition.

1. Introduction

Reverse microemulsion (such as "water in oil") is a thermodynamically stable system consisting of reverse micelles located in the nonpolar liquid [1–3]. Reverse micelles are nanoscale (1–100 nm) drops of water (water pool) or other polar solvent covered with a monolayer of surfactants (micelle shell). The size of water pools depends on the molar ratio of water and surfactants ($w = [H_2O]/[Surfactant]$) in reverse microemulsion. The properties of microemulsions determine a wide range of their applications in the food industry [4,5], in biomedicine [6–8], in the pharmaceutical and cosmetic industries [2,9]. Currently, reverse micelles are actively used as nanoreactors for obtaining monodisperse nanoparticles of a given size [3,10–14].

Typically, microemulsions contain 4 components: water, hydrocarbon, surfactant and co-surfactant (its addition allows to increase the amount of the dispersed phase of the liquid). However, some surfactants allow to create microemulsions without adding co-surfactants. These surfactants include AOT-Na (bis(2-ethylhexyl) sodium sulfosuccinate). Today, microemulsions with AOT are actively used in various nanotechnological and pharmaceutical processes [15–28]. In [15], it was shown that in the treatment of osteoporosis, using a transdermal system based on AOT microemulsion for the administration of alendronate provides a better pharmacokinetic profile compared to oral administration of the drug. Reverse AOT/water/heptane microemulsions are used for the synthesis of highly dispersed chitosan nanoparticles [16], for the extraction of α-lacalbumin [21] and other proteins [22–26]. AOT micellar structures in isooctane are widely used for protein bioregulation [27] and as traps for diethyl tartrate [28]. The use of reverse AOT micelles made it possible to modify and improve the thermal, textural, and some physicochemical properties of soy proteins [17]. Micellar solutions of AOT amphiphiles, sodium dodecyl sulfate (SDS), and cetyltrimethylammonium bromide (CTAB) were used for the synthesis of Au–Pd bimetallic nanoparticles [18]. Monodisperse copper nanoparticles were successfully synthesized in both forward and reverse AOT micelles [29]. In [19], magnetic nanoparticles coated with chitosan were obtained using reverse microemulsions of AOT-SDS. In [20], the authors showed that AOT/water/hexane microemulsions can be used as "sieves" for selecting and stabilizing J-aggregates of cyanine dye of the desired size.

The widespread use of AOT microemulsions requires active researches of the structure and solubilization properties of reverse AOT micelles. For the water/AOT-Na/cyclohexane microemulsion, it was found [30] that the more surfactants are dissolved in the oil phase, the more water can be contained inside the core of the formed reverse micelles. According to the results of the authors [31], in water/AOT/oil solutions, where cyclohexane, heptane, isooctane, dodecane, and toluene were used as oil, a sharp linear increase in the volume of solubilized

* Corresponding author.
E-mail address: plastinin_ivan@mail.ru (I.V. Plastinin).

https://doi.org/10.1016/j.molliq.2020.115153
0167-7322/

water is observed with an increase of the AOT concentration from 8 mM (mmol/kg). The authors explain this by the fact that at the concentration of 8 mM, reverse micelles with the constant micellar mass begin to form. These micelles can contain a much larger amount of water in their core, in contrast to small aggregates of surfactants, which are formed at AOT concentrations less than 8 mM. According to SANS (small-angle neutron scattering) data of authors [32], the first small aggregates of AOT in cyclohexane are formed already at AOT concentration of 0.225 mM. The authors [31] calculated the solubilization power of small associates and reverse micelles using a slope of straight sections of the dependence of the volume of solubilized water on the AOT concentration for different organic solvents. It turned out that the solubilization power at AOT concentrations up to 8 mM is the same for different oils, and at the same AOT concentrations in the region above 8 mM, the solubilization power increases sharply in the series: toluene < dodecane < isooctane < cyclohexane < heptane.

The behavior of reverse microemulsions of the water/AOT/oil type with the change of the parameter w ($w = [H_2O]/[AOT^-]$) is studied well [33–37]. According to the results of static and dynamic light scattering [33], in the water/$Ni^{2+}(AOT)_2$/cyclohexane system, one-dimensional growth of reverse micelles is observed with an increase of the parameter w, which leads to the fact that at $w = 6.3$ the micelles are elongated ellipsoids. The authors [34] studied the water/AOT/cyclohexane systems with a small amount of water ($w = 5$) using viscometry and small-angle neutron scattering. At the same time, AOT salts with various counterions were used as surfactants. A significant influence of the size of the counterion on the structure of reverse micelles was found. This influence is determined by the effective charge density on the counterion surface, which is proportional to the radius of the hydrated ion, and is manifested in the degree of curvature of the surface of the reverse micelle. In the limited volume of the polar micellar core with low water content, for large cations it is more difficult to approach the SO_3^- head groups than for cations with small sizes. It induces effective repulsions of SO_3^- groups from each other. Therefore, for small sizes of counterions (for example, Na^+) and small water content, the shape of micelles is spherical, and for large counterions, it is cylindrical.

In the article [35], reverse water/AOT-Na micelles were studied in three different organic solvents (cyclohexane, toluene, and chlorobenzene) by methods of measuring viscosity and dynamic light scattering. As results of using both methods linear dependence of the diameter of the reverse micelles on the parameter w was obtained: diameter increased from 3 to 5.5 nm with increasing w from 0 to 8. It was discovered that the size of the water pools was practically independent of solvent and concentration of AOT in oil. Similar conclusions were made by the authors [36,37]. The molar volume of water V_w calculated from density measurements in the water/AOT-Na/isooctane microemulsion at w values from 0 to 2 is small due to the strong interaction of water molecules with the ionic head groups of AOT [37]. For w in the range from 2 to 6, V_w increases due to weaker interactions of additional water molecules with the AOT head group and the growth of spherical reverse micelles. For values of w from 6 to 12, a complex non-monotonic course of the dependence of V_w on w is observed, which is associated by the authors with the rearrangement of micelles from spherical to non-spherical.

There are a number of articles in the literature on the study of reverse AOT microemulsions using vibrational spectroscopy [38–44]. It was established that the processes occurring in reverse micelles appear mostly in the behavior of the spectral band with the maximum at 1064 cm^{-1} in the Raman spectrum and in the area of 1051 cm^{-1} in IR spectrum at $w = 0$ (according to the authors [38], this band is caused by symmetric stretching vibrations of SO of sulfonate groups SO_3^-) and stretching band of OH-groups of water in the region 3400 cm^{-1}. As a result of analysis of IR absorption and Raman spectra of reverse microemulsions water/AOT-Na/isooctane and water/AOT-Na/cyclohexane, it was found that change of the w parameter from 0 to 15 leads to the shift of the SO stretching band in the Raman spectrum from 1064 to 1050 cm^{-1}, and in the IR absorption spectrum from 1051 to 1045 cm^{-1} [38]. The greatest shift of the bands is observed with increasing w from 0 to 3. For $w > 6$ there is only a slight shift, and if $w > 15$, the band does not shift. It is worth noting that the authors of [38] rely on the work [45] for interpretation of this band. However, as in the case of SDS [46], in addition to the symmetric stretching vibrations of SO_3 groups, there should be symmetric stretching vibrations of the C-C backbone in the 1060 cm^{-1} region. For example, the authors [47] assert that the band in the region of 1060 cm^{-1} belongs to the symmetric vibrations of C-C AOT. Therefore, we will not provide an explanation of the authors of the detected band shifts in terms of processes occurring in microemulsions.

In the study [39], reverse water/AOT/heptane microemulsions were studied by Raman spectroscopy. It was shown that when the water content in the microemulsion w increases from 2.4 to 58.6, the stretching band of water shifts to the region of smaller wavenumbers. In this case, the band itself turns from a bell-shaped band into a band with two maximums, similar to the stretching band of pure water. A similar shift of the water stretching band as a function of w in reverse AOT microemulsions is also observed in the IR spectra [40–44]. Representing the stretching band of water at each value of was a linear combination of the spectrum of "bound" water (the band at the lowest water content $w = 2.4$, when all water molecules are located near the head groups of AOT) and "bulk" water (the spectrum of pure water), the authors [39] found that with an increase of w from 2.4 to 20, the proportion of "bulk" water increases rapidly; for w from 20 to 40, the increase of the fraction of "bulk" water occurs very slowly. And after $w = 40$, the amount of "bulk" water begins to grow rapidly again. The authors assert that the growth of reverse micelles (for example, aggregation of water droplets) can occur in the region of $20 < w < 40$. The authors [42] used IR spectroscopy to show that water in the micelle core consists of "interphase "and "bulk" water. They showed that increasing w to 6 leads to significant changes in the OH stretching band, and when increasing w above 6, the OH band changes slightly, gradually becoming similar to the pure water stretching band.

As it was mentioned above, reverse microemulsions are in high demand in biotechnologies, pharmaceuticals, food processing, and nanotechnologies [3–5,10–12,14]. The characteristics of such systems directly affect the final product. For example, the shape and size of the synthesized nanoparticles are determined by the structure of the used reverse micelles. And the processes of reverse micelle formation, critical micelle concentration (CMC), and the structure of micelles, in turn, significantly depend on the amount and type of solvents, the ratio of their concentrations, the type and concentration of amphiphile, the temperature of the system, etc. Therefore, today there is an extremely great interest to the study of complex processes of self-organization of amphiphilic compounds in triple (or multicomponent) systems, in which reverse micelles of different sizes and shapes are formed.

Currently, there is no method of diagnostics of the processes of self-organization of amphiphiles that provides contactless sensing of multicomponent solutions of amphiphiles and allows working in real time. For example, in the synthesis of nanoparticles, in order to determine the size of the resulting particles, a number of actions should be performed: stop the synthesis reaction, change the temperature for particle deposition, wash the resulting particles with different solvents, centrifuge the mixtures, wash them again, dry them under vacuum, and only then one can characterize them - measure the size, evaluate the shape, etc. [48,49]. Thus, one can state that significant progress has been made in the application of micellar synthesis and micellar solubilization in various industries, in medicine, and in nanotechnology. However, contactless express diagnostics of processes and parameters of self-organization of amphiphiles in multicomponent solutions is not developed at all.

In this work, the processes of self-organization of surfactants in microemulsions were studied using laser Raman spectroscopy and method of dynamic light scattering (DLS) on the example of the

water/AOT-Na/cyclohexane system depending on the amount of solubilized water. The main regularities in the change in Raman spectra with changes of the size of reverse micelles have been established, which makes it possible to use laser spectroscopy as a promising express non-contact method for diagnostics of reverse microemulsions with aqueous core, in particular, for determining the size of micelles.

2. Materials and methods

2.1. Objects of research

For the preparation of reverse microemulsions the following reagents were used: AOT (bis (2-ethylhexyl) sodium sulfosuccinate $C_{20}H_{37}NaO_7S$, M=444.56 g/mol, Sigma-Aldrich, CAS:577-11-7, BioUltra, Purity: 99.6%), cyclohexane (C_6H_{12}, PanReac AppliChem, CAS:110-82-7, Purity: 99.9%), ultrapure deionized bidistilled water ("Millipore Simplicity UV" water filtration and purification system, water resistance 18.2 MΩ*cm at 25 °C).

The process of preparing reverse microemulsions water/AOT-Na/cyclohexane was carried out in several stages. First, a solution of 33.3 wt% AOT in cyclohexane (750 mM) was prepared. After complete dissolution, the resulting solution was poured into 14 separate vials. Then, such an amount of water was added to each solution that the parameter $w = [H_2O]/[AOT^-]$ changed from 0 (without water) to 11 with variable increment.

2.2. Methods of research

2.2.1. Raman spectrometer

The Raman signal was excited by the Laser Quantum Gem DPSS laser (532 nm wavelength, output power 500 mW). For suppression of elastic scattering an interference filter was used. It allowed approaching the laser excitation line up to 200 cm^{-1}. The spectra were recorded in 90° experiment geometry. A film polarizer was used to obtain the polarized and depolarized spectra. The detection system included monochromator (Acton, grating 1800 and 900 grooves/mm, focal length 500 mm) and CCD camera (Horiba Jobin Yvon, Syncerity). The registration time for one spectrum was 2 min. The spectral resolution in the region of the stretching band of water was 0.6 cm^{-1}. The processing of the spectra consisted of their correction for the laser power and spectral sensitivity of the registration system, baseline correction. The temperature of the samples was controlled by the KRIO-VT-01 thermal stabilization system and maintained constant at 25.0 ± 0.1 °C.

2.2.2. System of measuring the size of reverse micelles

The Malvern Zetasizer Nano–ZS light scattering analyzer (Malvern Instruments, UK) was used to determine the size of reverse micelles in the studied samples. In Zetasizer series of laser analyzers, the size of particles and molecules is measured by DLS method in the range from 0.3 nm to 10 μm. The measurement accuracy according to the manufacturer's data is ±2%. The temperature of the samples was maintained at 25.0 ± 0.1 °C.

In experiments the size of the reverse micelle for each studied microemulsion was determined 3–5 times by DLS method, and then the arithmetic mean value of d and its standard deviation were calculated. For more information, see Suppl. Material, paragraph 1.

3. Results and discussion

3.1. Determination of the size of reverse micelles in the studied samples

The DLS method was used for determination of the size of reverse micelles in all the studied water/AOT-Na/cyclohexane microemulsions. For samples with w from 0 to 5, the autocorrelation function was well described by single exponent, but for samples with w > 6, one exponent was not enough for approximation. This may be caused by the fact that at w > 6, the reverse micelles begin to strongly bend and stretch, their shape is transformed from spherical to ellipsoid. These results are in good agreement with the data [33,37]. Thus, according to our data, the region where reverse micelles have spherical shape in the studied water/AOT-Na/cyclohexane microemulsions lies in the range of w values from 0 to 5. The obtained dependence of the diameter of spherical reverse micelles d on the parameter w is shown in Fig. 1.

As the water content in the microemulsion increases, the size of water droplets solubilized in reverse AOT micelles increases, thereby increasing the size of the micelles themselves. The dependence of the diameter of the reverse micelles d on w (Fig. 1) is approximated with good accuracy by the linear function in the range w from 0 to 5 (the approximation parameters are shown in Fig. 1). The linear increase of the size of reverse micelles with an increase of the water content when w changes from 0 to 5 is consistent with the data [35].

3.2. Raman spectroscopy of reverse microemulsions of AOT

Unpolarized spectra (which include the contribution of the polarized and depolarized Raman signals), polarized, and depolarized Raman spectra of all samples were obtained in a wide range of wavenumbers - from 200 to 4500 cm^{-1}. Fig. 2 shows the unpolarized Raman spectra of cyclohexane, water, and the water/AOT/cyclohexane microemulsion with w = 0 and 11.

In the Raman spectrum of cyclohexane, the following most intense bands are observed: CC stretching vibrations with maximums near 805 and 1034 cm^{-1}, bending vibrations of CH_2-groups (rocking vibrations with maximum near 1163 cm^{-1}, twisting vibrations −1274 cm^{-1}, wagging vibrations - 1354 cm^{-1}, scissoring vibrations - 1450 cm^{-1}) and CH stretching vibrations in the region 2800–3000 cm^{-1} [50] (Fig. 2). The bands of stretching vibrations of CH groups CH_3 AOT are also located in the region 2800–3000 cm^{-1}, in the region 1100–1500 cm^{-1} there are bands of bending vibrations of CH_2 of groups CH_3; near 1060 cm^{-1} one can observe band which can be caused symmetric stretching vibrations of SO_3 groups, SO, and SS stretching vibrations of hydrocarbon radicals AOT [45–47] (Fig. 2). In the Raman spectrum of water, the most intense and very broad OH stretching band is located in the region 3000–3700 cm^{-1} [51–53] (Fig. 2). In addition, the Raman spectrum of water contains band of vibrations with combination frequencies of OH groups (3800–4300 cm^{-1}), association band (1900–2400 cm^{-1}), bending band (1500–1800 cm^{-1}), broad band of intermolecular translational and libration vibrations (300–1100 cm^{-1}), and weak bands of intermolecular vibrations of hydrogen bonds (50–300 cm^{-1}) located on the intense Rayleigh scattering shoulder [52,54,55].

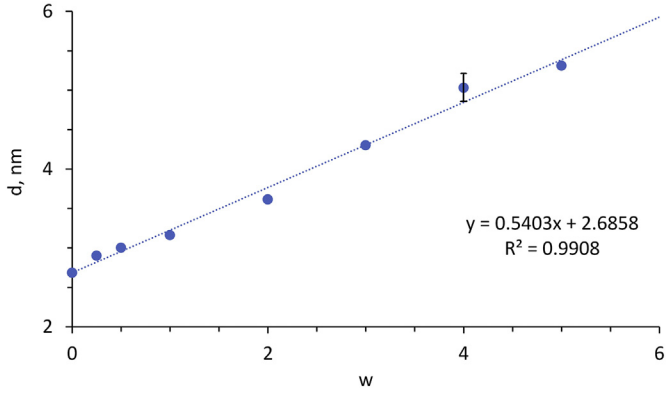

Fig. 1. Dependence of the diameter of reverse micelles d on w. The size measurement error is 4%.

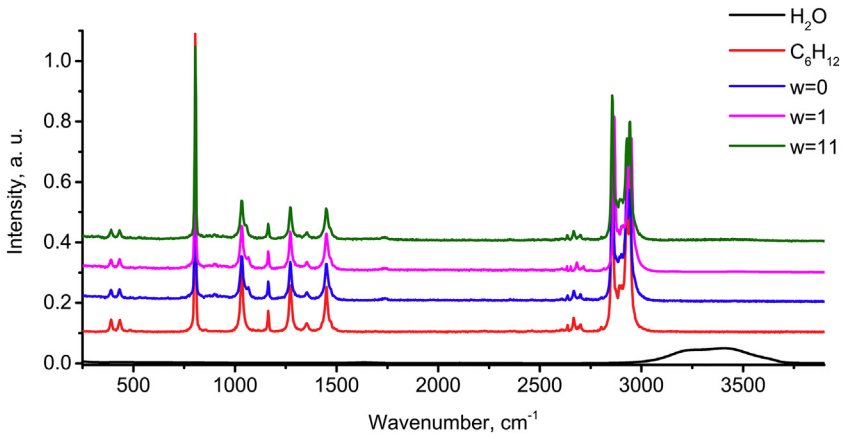

Fig. 2. Unpolarized Raman spectra of water, cyclohexane C_6H_{12} and microemulsions with w = 0, 1 and 11. For clarity, each upper spectrum is shifted by 0.1 in intensity up relative to the lower one.

3.2.1. Dependence of the spectral characteristics of the OH stretching band of water (3100–3700 cm^{-1}) solubilized in the core of reverse micelles on w

In order to analyze the stretching bands of water, the separation of contribution of water to the Raman spectrum of the microemulsion was performed for each sample with w > 0. For this purpose, difference spectra were constructed: the spectrum of AOT and cyclohexane (sample with w = 0) was subtracted from the Raman spectrum of the microemulsion (each sample with w > 0). Fig. 3a shows the unpolarized spectra of cyclohexane and microemulsions with w = 0, 11, and Fig. 3b shows the difference spectra for all studied w, normalized by the area of the OH stretching band. Similarly, polarized and depolarized stretching bands of OH of water in microemulsions were obtained (Fig. S1, S2).

As it can be seen from Fig. 3b and S1b, as the amount of solubilized water increases, the shape of the water stretching band changes significantly: with increasing w, the intensity of the low-frequency region of band increases, and the intensity of high-frequency region of band decreases, and the band itself shifts towards low frequencies. For assessment of changes in the position and shape of the water stretching band the following values were used: the position of the maximum of the band ν_{max}, the position of center of mass $\nu_{c.m.}$, FWHM $\Delta\nu$ (full width at half maximum) and parameter χ_{21} (the ratio of the intensity of high-frequency (I_{3500} cm^{-1}) shoulder of the band to the intensity of low-frequency shoulder (I_{3300} cm^{-1}), i.e. $\chi_{21} = I_{3500}/I_{3300}$) (Fig. 3b) [56]. The position of the center of mass was determined as follows:

$$\nu_{c.m.} = \frac{\sum_i I_i \cdot \nu_i}{\sum_i I_i} \quad (1)$$

where I_i - intensity at frequency ν_i.

For all studied samples, the dependences of the specified spectral characteristics on the parameter w were constructed (Fig. 4). Similarly, such dependences were constructed for polarized (Fig. S3) and depolarized OH stretching bands (Fig. S4).

For explanation of the obtained dependences (Fig. 4) we decomposed the OH stretching band of each studied microemulsion into 5 components that correspond to a certain local structure of the hydrogen bonds of the H_2O molecule: DAA, DDAA, DA, DDA (water molecules can act as a proton donor (D) and proton acceptor (A) (see Fig. 5a)) and free (weakly bound/unbound water molecules) [57–59].

In order to isolate components from a wide stretching band of water, the method of genetic algorithms in combination with the gradient descent method was used [53,60–62]. The components of the decomposition of the Gaussian shape were chosen. Decomposition was carried out for three spectra of each microemulsion, after which the average values and standard deviations of the parameters of components were calculated. The results of decomposition are shown in Fig. 5.

As it can be seen from Fig. 4a, the dependence ν_{max}(w) can be approximated well by two straight lines intersecting at the point w = 5. This stepwise shift of the position of maximum of the stretching band

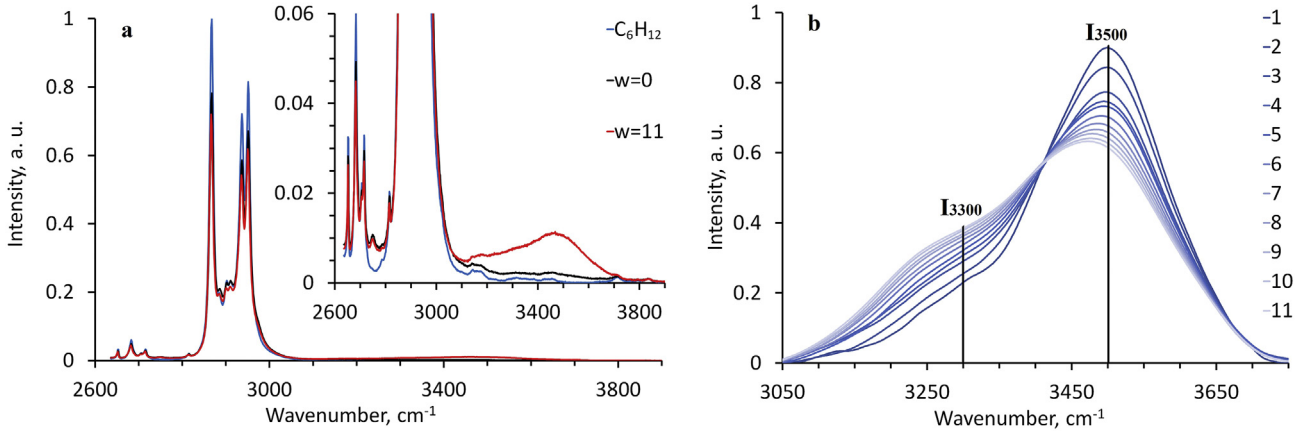

Fig. 3. Unpolarized Raman spectra of cyclohexane and microemulsions with w = 0 and 11 (a); Unpolarized bands of stretching vibrations of OH of water in microemulsions with different water content (various values of w) (b).

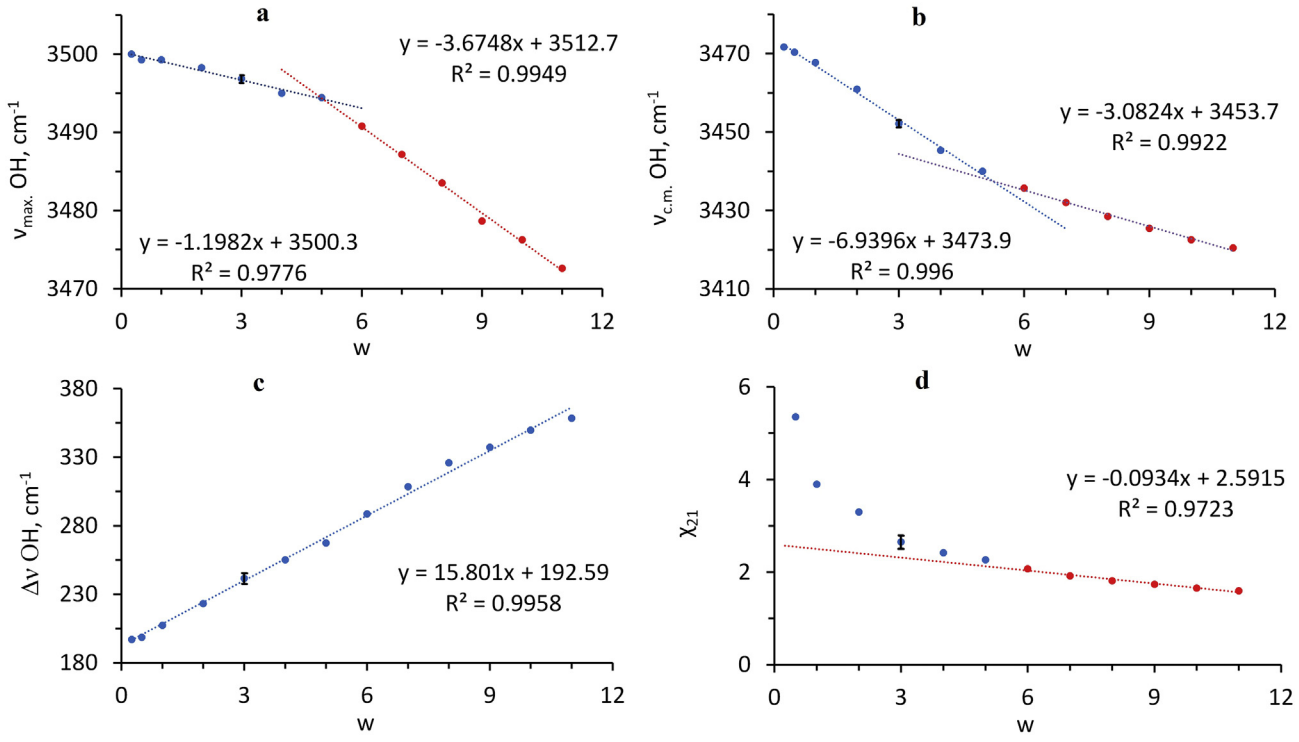

Fig. 4. Dependences of the position of maximum (a), center of mass (b), FWHM (c), and parameter χ_{21} (d) for unpolarized OH stretching bands on the amount of solubilized water in reverse micelles of microemulsion (w).

of water towards smaller wave numbers with increasing w (Fig. 4a) shows that for w ≤ 5, the frequency of stretching vibrations decreases very slowly for most water molecules (the blue linear section in Fig. 4a). At the same time, about 70% of the intensity of the entire OH band is caused by water molecules bound by a single pair of donor-acceptor (DA) hydrogen bonds (component 3 in Fig. 5b). For w > 6, the frequency of stretching vibrations decreases about 3 times faster with increasing w than for small w (the red linear section in Fig. 4a). Meanwhile the contribution of molecules with DA bonds became smaller, and the contribution of molecules with DDAA bonds - greater (components 2 and 3 in Fig. 5b). This means an increase of the connectivity of water molecules in the core of the reverse micelle with increase of the water content. Thus, the connectivity of most of the water molecules in the water core increases gradually to w = 5, and at large w their connectivity increases much faster (Fig. 4a) (an increase in connectivity means an increase in the number and strength of bonds per water molecule [52]). Such a sharp change in the dynamics of the binding of water molecules, which leads to the break in the region w = 6 (Fig. 4a, Fig. 5b), suggests that when the ratio of the number of water molecules to the number of AOT anions is approximately 6:1, an internal rearrangement of the core of the reverse micelle occurs. At w = 6, the number of water molecules is 6 times greater than the number of Na^+ counterions. At this ratio, water molecules can form hydrate shell around Na^+ cations [34,63], thereby shielding them from the SO_3^- AOT head groups. After that, the water molecules added to the solution again (i.e. at w > 6) will be able to form strong

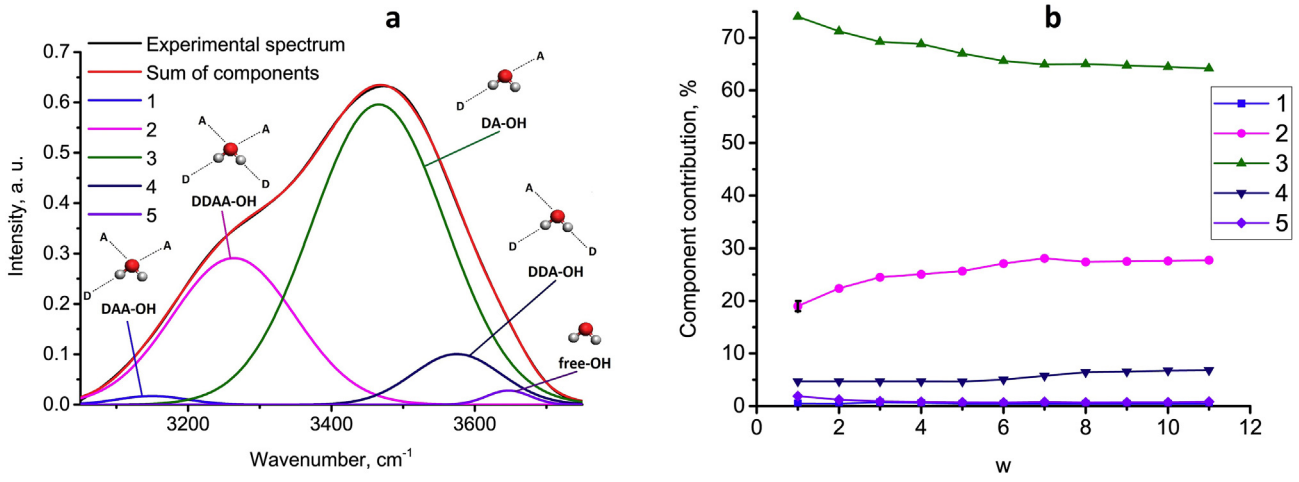

Fig. 5. Decomposition of the OH stretching band of the microemulsion (w = 11) into 5 components of the Gaussian shape (a), the dependence of the relative contribution of each component to the intensity of the OH stretching band (b) on the parameter w.

hydrogen bonds with SO_3^- groups, which will not be hindered by hydrated Na^+ ions.

The formation of hydrogen bonds with groups SO_3^- if w > 6 is confirmed by the course of dependence of the contribution of component 4 on w presented in Fig. 5b. As the water molecules form hydrogen bond with the oxygen atom of the group SO_3^- acting as donor of proton (D) (i.e., DA bond of water molecule transforms to DDA bond). One can observe an increase of contribution of component 4 (DDA) and decrease of the contribution of component 3 (DA) with increasing w from 6 to 11 (Fig. 5b).

As it can be seen from Fig. 4b, the dependence of the center of mass of $\nu_{c.m.}$ on the parameter w as well as the dependence $\nu_{max}(w)$, can be approximated well by two straight lines intersecting at the point w = 5.3. Such a small change in w in the point of intersection of lines can be explained by the fact that this dependence $\nu_{c.m.}$ (w) shows how change of w changes the average connectivity not of the most part of water molecules but of all water molecules present in the cores of reverse micelles. In this case, the average connectivity of water molecules increases faster with an increase of w from 0 to 5 (the blue linear section in Fig. 4b, components 2 and 3 in Fig. 5b), than when increasing w from 6 to 11 (red linear section in Fig. 4b). This clearly demonstrates the change of the form of band with change of parameter w (Fig. 3b): with increasing w from 0.25 to 5, there is a significant change of the band shape compared with that for large values of w. The described dynamics of the binding of OH groups of water molecules in the core of the reverse micelle with an increase of w is confirmed by the dependence of the parameter χ_{21} on w (Fig. 4d) By its definition, the parameter χ_{21} is equal to the ratio of the number of weakly bound groups of water molecules to strongly bound ones (see above, [56]). That is why the course of the obtained dependence $\chi_{21}(w)$ indicates that for small values of w, the proportion of weakly bound OH groups of water molecules in reverse micelles of AOT at first decreases sharply (that is, the number of strongly-bound OH groups actively increases (component 2 in Fig. 5b)), at w ~ 4 this reduction is slowed down (the number of strongly-bound groups OH grows slower), and when w > 5 there is a relative balance between the weakly- and strongly-bound water molecules (the dependence $\chi_{21}(w)$ is approximated by straight line), although the proportion of weakly bound OH groups continues to decrease (Fig. 4d, components 2 and 3 in Fig. 5b).

The dependence of the FWHM of the water stretching band $\Delta\nu$ on w is shown in Fig. 4b. In contrast to all other characteristics, the FWHM increases monotonically with increasing w (Fig. 4 a,b,d), and the dependence $\Delta\nu$ (w) in the entire studied range w is approximated well by straight line. The band broadening is explained by the increase of the number of strongly bound OH groups of water molecules in the core of the reverse micelle when water is added to the microemulsion. Namely the stretching vibrations of strongly bound OH groups give their contribution to the Raman spectrum in the region 3200–3300 cm^{-1}. When w changes from 0.25 to 11, the FWHM of the stretching band of water increases by 2 times. Another reason for this broadening may be Fermi resonance: an increase of the binding water molecules may increase the resonant interaction between the symmetric stretching vibration OH and the overtone of the bending vibration H-O-H, which may lead to even greater band broadening [60,61].

The dependences of the position of the maximum, center of mass, FWHM, and χ_{21} on the parameter w obtained for polarized spectra almost completely repeat the behavior of the corresponding dependences for unpolarized spectra (Fig. S3). At the same time, there are significant differences for depolarized spectra. Changes of the position of the maximum and center of mass are not as significant as for unpolarized and polarized spectra: when w increases from 1 to 11, the position of maximum decreases by 10 cm^{-1} (for unpolarized and polarized - almost 30 cm^{-1}), and the center of mass shifts by about 15 cm^{-1} (against 50 cm^{-1}) (Fig. S4). For depolarized spectra, there is no sharp break in the dependences $\nu_{max}(w)$ and $\nu_{c.m.}$ (w) at w = 5–6 (Fig. S4), and the FWHM also changes linearly with increasing w, but only by 15%, not by 2 times (Fig. S4).

The obtained results indicate a high sensitivity of the OH stretching band to the amount of water solubilized in the reverse micelle, and, consequently, to the size of the reverse micelle. At the same time, at w = 6, when water molecules hydrate/shield Na^+ cations, so that water molecules can now closely approach the SO_3^- AOT head groups and form strong hydrogen bonds with them, such an effect of water molecules on the micelle shell of AOT anions from the inside of the micelle core does not remain without consequences. Micelles begin to change their shape from spherical to more elongated (ellipsoidal or cylindrical). This transformation of micelles just begins to occur at w > 6, which is confirmed by our data obtained by the DLS method and data from other authors [33]. The sensitivity of the OH stretching band makes it possible to detect this transformation using Raman spectra (Fig. 4).

3.2.2. Influence of water solubilization on the AOT spectral band in the region 1040–1080 cm^{-1}

Fig. 6a shows the unpolarized spectra of cyclohexane and microemulsions with w = 0, 3, 6, 11 in the region 1000–1100 cm^{-1}. The band with a maximum near 1034 cm^{-1} corresponds to the stretching vibrations of the CC cyclohexane backbone, and in microemulsions on its shoulder there is AOT band, which some authors associate with the stretching vibrations of CC AOT backbone [47], and

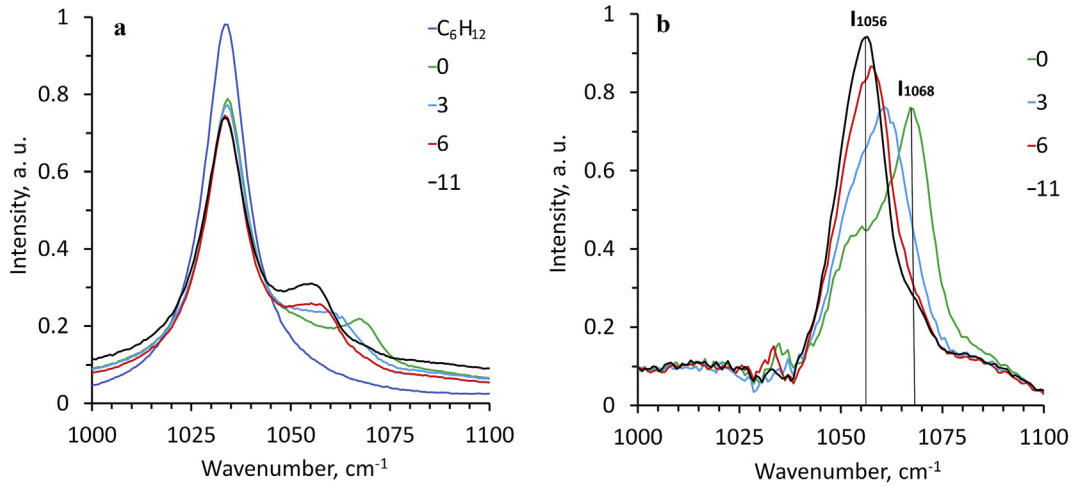

Fig. 6. Unpolarized Raman spectra of cyclohexane and microemulsions with w = 0, 3, 6, 11 (a); difference spectra at w = 0, 3, 6, 11 (b).

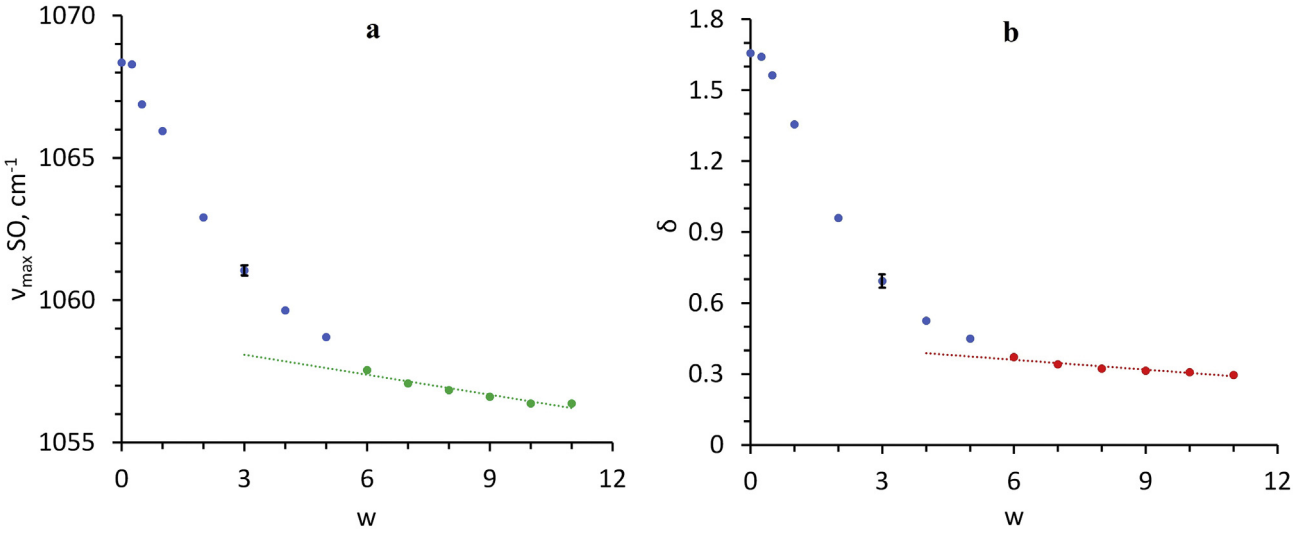

Fig. 7. Dependences of the position of maximum (a) and the ratio of the intensities $\delta = I_{1068}/I_{1056}$ (b) of the difference spectra of the AOT band on the parameter w for the unpolarized spectra of microemulsion.

others with the stretching vibrations of the SO sulfonate group SO_3 of AOT [45]. As it can be seen from Fig. 6a, this band is very sensitive to changes of the amount of solubilized water. In order to analyze the behavior of this band, difference spectra were obtained: the spectrum of cyclohexane in the studied region was subtracted from the microemulsion spectrum. The difference spectra of the same samples with w = 0, 3, 6, 11 are shown in Fig. 6b.

As it can be seen from Fig. 6b, when w = 0, the AOT band has a two-humped shape with the maximum at 1068 cm^{-1} and intense shoulder at 1056 cm^{-1}. As the amount of solubilized water in the micelle core increases, the band shape begins to change: the maximum shifts to the left, and the low-frequency shoulder becomes more intense. At w = 11, the maximum is already in the area of 1056 cm^{-1}, and to the right of the maximum there is only a small shoulder in the area of 1068 cm^{-1}. In order to quantify these changes, parameter δ was introduced, which equals the ratio of intensities of high-frequency shoulder (I_{1068}) of AOT band in the region 1040–1110 cm^{-1} to the intensity of low-frequency shoulder (I_{1056}) (Fig. 6). The dependences of the position of the band maximum and the intensity ratio $\delta = I_{1068}/I_{1056}$ on the parameter w were constructed (Fig. 7).

In order to explain the obtained dependences (Fig. 7), we decomposed the AOT bands in the region of 1040–1110 cm^{-1} of each of the studied microemulsions into 3 components of the Gaussian shape (Fig. 8a):

We assume that component 1 with maximum near 1056 cm^{-1} corresponds to the stretching vibrations of SO of bound SO_3 groups, component 2 with maximum near 1068 cm^{-1} corresponds to the stretching vibrations of unbound SO_3 groups, and the component 3 with maximum near 1081 cm^{-1} probably corresponds to CC vibrations (the width of this component is associated with a variety of different CC bonds in the AOT anion). As it can be seen from Fig. 8b, the area of component 3 practically does not change with the addition of water, since the concentration of AOT remains almost constant, which confirms our assumption that component 3 corresponds to CC vibrations. The areas of components 1 and 2 change significantly with increase of w from 0 to 3, change slightly with increase of w from 3 to 6, and practically do not change for w > 6 (Fig. 8b). This means that as w increases, the number of strongly bound SO_3 groups increases and the number of weakly bound groups decreases. This change in the ratio of contributions of components 1 and 2 actually confirms the explanation of the corresponding change of the parameter δ with increasing w (Fig. 7b).

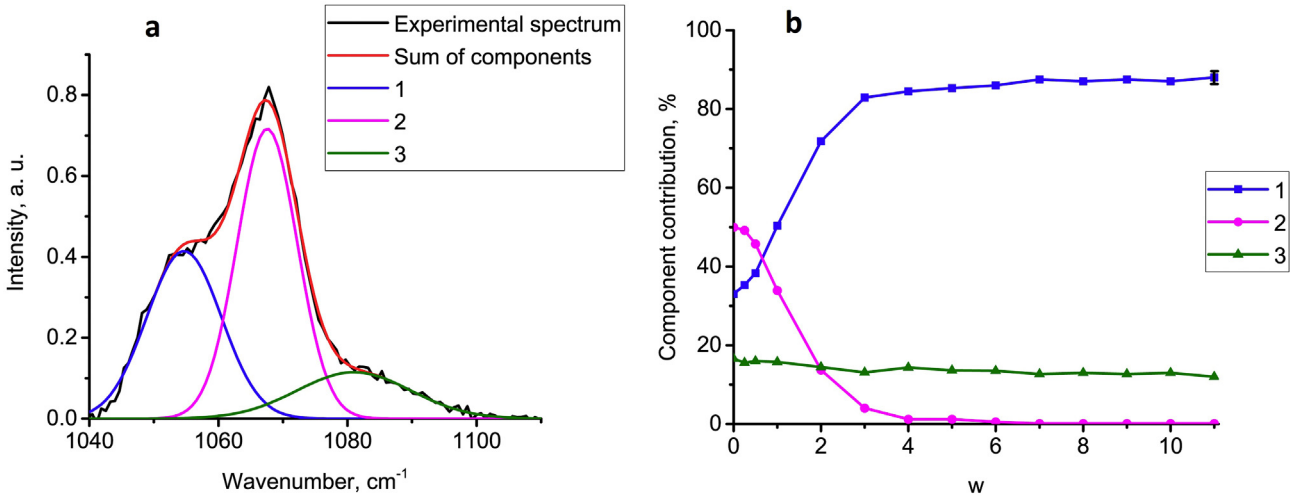

Fig. 8. Decomposition of the AOT band in the region 1040–1110 cm^{-1} of the microemulsion (w = 11) into 3 components of the Gaussian shape (a), the dependence of the relative contribution of each component to the intensity of the SO stretching band (b) on the parameter w.

Fig. 7a shows that when the amount of water in the microemulsion increases, the maximum of the studied band shifts sharply to the low frequency region, but the shift slows down when w approaches 6, and when w > 6, the shift occurs linearly, which corresponds to the the dependencies of component contributions (Fig. 8b). The dependence δ(w) shows that at w < 6, the intensity of the high-frequency region of the band decreases rapidly, while the intensity of low-frequency region, on the contrary, increases. As the w value approaches 6, these processes slow down (Fig. 7b, Fig. 8b). For w > 6, the dependence δ(w) becomes linear. This shift of the band and the change in the relative intensity $\delta = I_{1068}/I_{1056}$ with increasing w can be explained if one assumes that the main contribution to the studied band is made by the stretching vibrations of the SO group SO_3, which is confirmed by the data of decomposition (Fig. 8b). The contribution to the 1068 cm^{-1} region is caused by weakly bound head group (i.e., the SO_3 group that does not interact well with water and does not form strong hydrogen bonds), and the contribution to the 1056 cm^{-1} region is caused by strongly bound SO_3 groups (Fig. 8). In this case, as the amount of water increases from 0 to w = 6, water molecules gradually hydrate/shield the Na^+ counterion and form stronger hydrogen bonds with the SO^3 head group, thereby shifting the frequency of SO stretching vibrations from 1068 cm^{-1} to 1056 cm^{-1} (at the same time, the number of bound groups increases dramatically SO_3 (Fig. 8b)). When there are enough water molecules to completely hydrate the Na^+ ions (w = 6, i.e. 6 H_2O molecules per 1 Na^+ cation), nothing prevents the water molecules from forming hydrogen bonds with the AOT head group. Therefore, as soon as all cations are surrounded by hydrate shells, the SO stretching band begins to shift to low frequencies very slowly, most likely due to the strengthening of existing hydrogen bonds.

Thus, analysis of the behavior of the AOT band caused by stretching vibrations of SO_3 groups showed that this band, like the OH stretching band of water, is very sensitive to changes of the amount of water solubilized in the core of reverse micelles. It was found that when w = 6 there is a sharp change in the course of dependency of spectral features both of OH band (Fig. 4) and SO band (Fig. 7), caused by the formation of hydration shells of the counterions Na^+ and, consequently, transformation of the form of reverse micelles from spherical to nonspherical. Hydration of Na^+ counterions allows water molecules and the head groups of SO_3 AOT to interact directly, which is shown in the spectra of stretching vibrations of these groups (OH and SO).

3.3. Method of determination of the size of reverse micelles in AOT microemulsions using laser Raman spectroscopy

The results of laser Raman spectroscopy of reverse water/AOT-Na/cyclohexane microemulsions presented above showed a high sensitivity of the OH and SO stretching bands to changes of the amount of solubilized water, which in turn affects the size of the reverse micelles. Taking into account this sensitivity of the specified spectral bands of the water/AOT/cyclohexane microemulsion, the relationship of their characteristics with the sizes of the corresponding micelles obtained by the DLS method was established.

The calibration curves of the position of the maximum, center of mass, and FWHM of the stretching bands of OH groups of water on the size of the reverse micelles were constructed. Fig. 9 shows these calibration curves for the unpolarized stretching band of OH groups of water.

As it can be seen from Fig. 9, the course of all calibration curves is linear. This is not surprising, since the dependence of the position of the maximum, center of mass, and FWHM of the unpolarized stretching band of OH groups of water on w (Fig. 4) and the dependence of w on the size of micelles (Fig. 1) are linear in the area corresponding to spherical reverse micelles (up to w = 6). Basing on the obtained calibration curves (Fig. 9), one can estimate the size of reverse micelles in the microemulsion with the following accuracy: the greatest accuracy is given by the calibration curve of the position of the maximum of the OH stretching band on d - 4.4%; the calibration curve of the position of the center of mass on d provides an accuracy of 4.5%, and the calibration curve of the FWHM on d - 5.3% (Table 1). A detailed description of the error calculation is provided in Suppl. Material (pp.1,2). It should be noted, that when calculating these values of accuracy of determination of the size of the reverse micelles, the accuracy of approximation of dependences and accuracy of DLS method were taken into account.

Since the shape of the unpolarized spectra depends to a large extent on the specific experimental setup, in contrast to polarized and depolarized spectra, similar calibration curves were constructed for these spectra (Fig. S5, S6). It was found that when determining the size of micelles from Raman spectra, the best results were achieved using unpolarized Raman spectra. However, in some situations it can be more simple and convenient to use, for example, polarized spectra. Therefore, the corresponding calibration curves are given in Suppl. Material. The obtained calibration curves of the position of maximum, center of mass, and FWHM of the stretching band of OH groups of water on w for polarized (Fig. S5) and depolarized (Fig. S6) spectra were approximated by straight lines. Similarly to the method described above, the

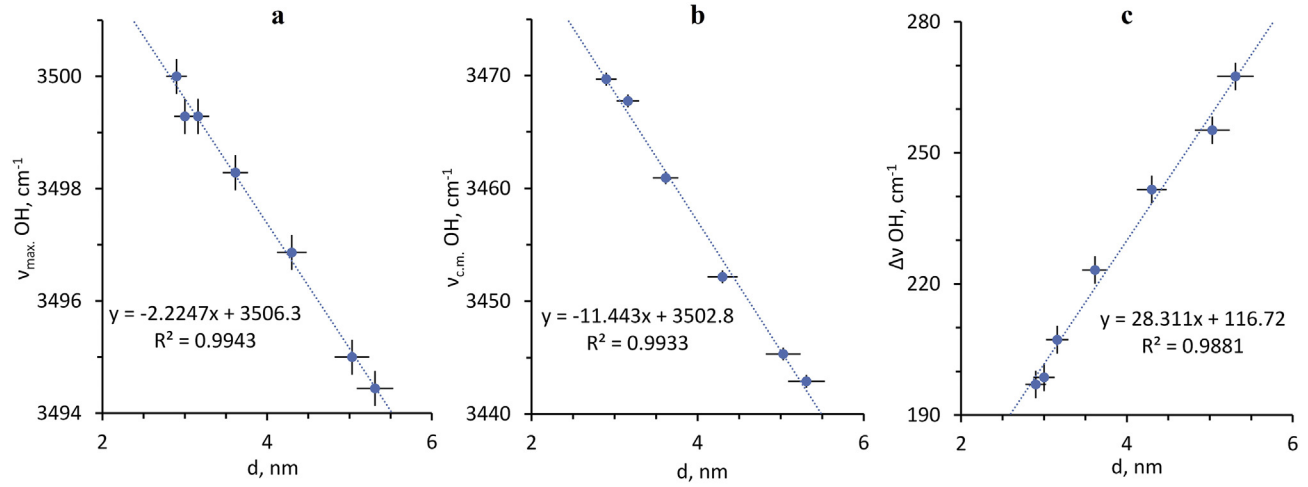

Fig. 9. Calibration curves of the position of the maximum (a), center of mass (b), and FWHM (c) of the unpolarized stretching band of OH groups of water on the size of reverse micelles.

Table 1
Accuracies of determination of the size of reverse micelles in the water/AOT/cyclohexane microemulsion using calibration curves of the spectral characteristics of the OH and SO group stretching bands on the size of micelles d.

Method of determination	Error, %		
	Unpolarized	Polarized	Depolarized
Calibration curve of the position of maximum of OH stretching band (3100–3700 cm^{-1}) on d	4.4	5.1	6.1
Calibration curve of the position of center of mass of the OH stretching band (3100–3700 cm^{-1}) on d	4.5	5.8	5.0
Calibration curve of the FWHM of the OH stretching band (3100–3700 cm^{-1}) on d	5.3	7.5	4.9
Calibration curve of the position of maximum of the SO_3 stretching band (1040–1080 cm^{-1}) on d	19		
Calibration curve of the ratio of intensities $\delta = I_{1068}/I_{1056\ of}$ of SO_3 stretching band (1040–1080 cm^{-1}) on d	13		

accuracy of determining the size of micelles from the constructed calibration curves was estimated. All obtained values of the accuracy of measuring the size of reverse micelles by calibration curves are shown in Table 1.

The calibration curves of maximum position and the intensity ratio $\delta = I_{1068}/I_{1056}$ of the AOT spectral band due to stretching vibrations of SO_3 groups on the size of reverse micelles d are shown in Fig. 10.

The course of the obtained calibration curves (Fig. 10) can be worse described by the linear law in comparison with the calibration curves for the OH stretching band (Fig. 9). Therefore, the approximation was carried out using second degree polynomial. This leads to large errors in determining the size of reverse micelles when using these calibration curves. The greatest accuracy is given by the calibration curve of the position of the maximum of SO band on d - 19%, and the calibration curve δ(d) allows one to determine the size of reverse micelles with accuracy 13% (Table 1). A detailed description of the error calculation is given in the Suppl. Material (pp. 1,2).

All the obtained accuracies of determination of the size of reverse micelles using the calibration curves of the spectral characteristics of the unpolarized, polarized, and depolarized stretching bands of OH groups and unpolarized stretching bands of SO_3 groups of Raman spectra of AOT microemulsions on the size of micelles are shown in Table 1.

As it can be seen from Table 1, the greatest accuracy in determining the size of reverse micelles is provided by the calibration curve of the position of the maximum of the unpolarized stretching band of water on the size of reverse micelles d. It is 4.4%. At the same time, the main contribution to this error is caused by inaccuracy of determining the sizes themselves by the DLS method: in our experiments, the average error of determination of the sizes was 4%. However, as it was mentioned earlier, from the point of view of spectrum registration, unpolarized spectra are not completely universal. Therefore, calibrations were made for polarized and depolarized stretching bands of OH groups, which provide errors slightly higher - from 4.9 to 7.5%. This is caused by lower intensity of these bands compared to the intensity of the unpolarized band. The use of calibration curves of the spectral characteristics of the SO_3 stretching band on the size of micelles d gives the size measurement error from 13 to 19%. This is mainly caused by the location of this band on the shoulder of the CC cyclohexane stretching band, which leads to the less accurate calculation of the values of the spectral characteristics of the SO_3 stretching band.

Thus, it is possible to determine the size of reverse micelles in the microemulsion with good accuracy using Raman spectral bands of water/AOT/cyclohexane microemulsion. At the same time, the errors in determining the size of micelles can be comparable to those of the most common method of measuring sizes – DLS. In addition, the method of laser Raman spectroscopy has undeniable advantages over other contact methods: it can be implemented in remote mode and it is not time-consuming. Namely Raman spectroscopy allows non-contact real-time diagnostics of micellar media, for example, measurement of critical micelle concentrations and concentration of formation of pre-micellar associates, determination the transformation of micelles from spherical to non-spherical. We developed these methods for direct micelles in double and triple systems: in aqueous solutions of sodium octanoate [52] in aqueous and water-ethanol solutions of sodium dodecyl sulfate [46,62]. In this paper, we have shown that laser Raman spectroscopy can be used for determination of the size of reverse micelles and obtaining information about their shape.

In this work, laser Raman spectroscopy was applied to water/AOT/cyclohexane microemulsions. However, if one takes into account that the processes occurring with water molecules in the water core of the reverse AOT micelle are common for other continuous oil phases (for example, hexane, heptane, isooctane), then one can assert that the proposed method is universal for such systems. This conclusion is confirmed by our results of studies of aqueous solutions of sodium octanoate and water-ethanol solutions of sodium dodecyl sulfate [46,52,62] using laser Raman spectroscopy. In these studies, despite different surfactants and solvents, general patterns of behavior of the spectral bands of water and surfactants were observed.

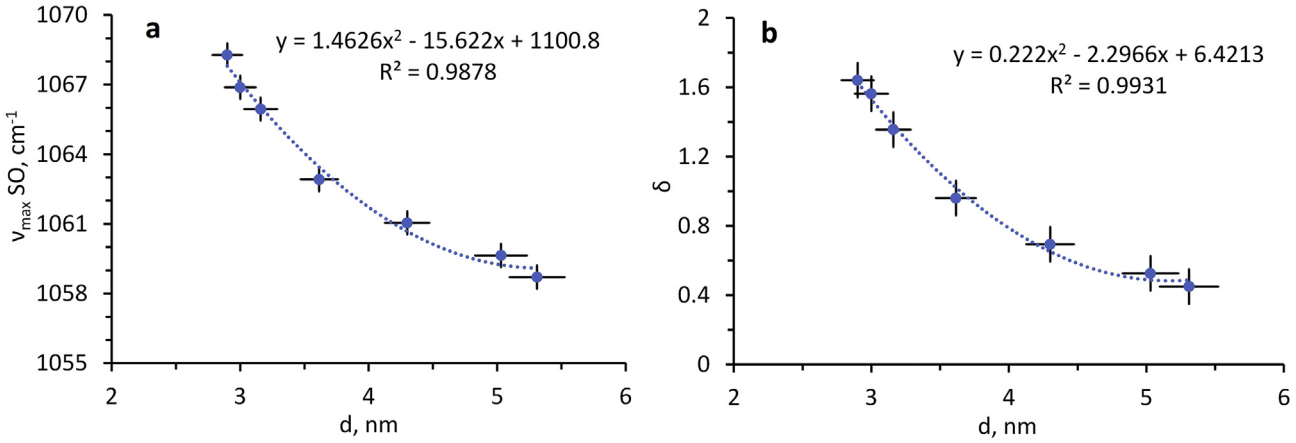

Fig. 10. Calibration curves of the position of maximum of the SO_3 stretching band (a) and the intensity ratio $\delta = I_{1068}/I_{1056}$ (b) on the size of the reverse micelles.

4. Conclusions

As a result of studying the processes of self-organization of AOT-Na in the reverse microemulsion water/AOT/cyclohexane using Raman laser spectroscopy, it was found that the bands of water and surfactants are extremely sensitive to the size and shape of reverse micelles. It was proposed to use this sensitivity of the stretching bands of the OH and SO groups of the Raman spectrum of microemulsions for elaboration of the method of determination of the size using Raman spectra. For determination of the size of micelles, calibration curves of the spectral characteristics of these bands on the size of the reverse micelles were obtained. It was shown that the developed method can provide the best accuracy of determining the size of spherical reverse micelles 4.4%. The proposed method of laser diagnostics of microemulsions can also be applied to microemulsions with different composition.

Authorship contribution statement

Plastinin Ivan V.: Conceptualization, Methodology, Validation, Formal analysis, Investigation, Writing - Original Draft, Writing - Review & Editing. **Burikov Sergey A.**: Resources, Writing - Original Draft, Writing - Review & Editing, Investigation. **Dolenko Tatiana A.**: Conceptualization, Resources, Writing - Original Draft, Writing - Review & Editing, Project administration.

Declaration of Competing Interest

None.

Acknowledgement

This study has been performed at the expense of Russian Science Foundation, project no. 19-11-00333 (I.V.Plastinin, T.A.Dolenko – Raman spectroscopy experiments, the application of machine learning methods) and by the Interdisciplinary Scientific and Educational School of Moscow University «Photonic and Quantum Technologies. Digital Medicine» (S.A.Burikov – DLS measurements).

Appendix A. Supplementary data

Supplementary data to this article can be found online at https://doi.org/10.1016/j.molliq.2020.115153.

References

[1] G. Tartaro, H. Mateos, D. Schirone, R. Angelico, G. Palazzo, Microemulsion microstructure(s): a tutorial review, Nanomater 10 (2020), https://doi.org/10.3390/nano10091657.
[2] S. Chen, S. Hanning, J. Falconer, M. Locke, J. Wen, Recent advances in non-ionic surfactant vesicles (niosomes): fabrication, characterization, pharmaceutical and cosmetic applications, Eur. J. Pharm. Biopharm. (2019), https://doi.org/10.1016/j.ejpb.2019.08.015.
[3] M. Jalali-Jivan, F. Garavand, S.M. Jafari, Microemulsions as nano-reactors for the solubilization, separation, purification and encapsulation of bioactive compounds, Adv. Colloid Interf. Sci. 283 (2020) 102227, https://doi.org/10.1016/j.cis.2020.102227.
[4] M. Jalali-Jivan, S. Abbasi, Novel approach for lutein extraction: food grade microemulsion containing soy lecithin & sunflower oil, Innov. Food Sci. Emerg. Technol. 66 (2020) 102505, https://doi.org/10.1016/j.ifset.2020.102505.
[5] M.D. Chatzidaki, F. Balkiza, E. Gad, V. Alexandraki, S. Avramiotis, M. Georgalaki, V. Papadimitriou, E. Tsakalidou, K. Papadimitriou, A. Xenakis, Reverse micelles as nano-carriers of nisin against foodborne pathogens. Part II: the case of essential oils, Food Chem. 278 (2019) 415–423, https://doi.org/10.1016/j.foodchem.2018.11.078.
[6] M.A. Momoh, K.C. Franklin, C.P. Agbo, C.E. Ugwu, M.O. Adedokun, O.C. Anthony, O.E. Chidozie, A.N. Okorie, Microemulsion-based approach for oral delivery of insulin: formulation design and characterization, Heliyon 6 (2020) e03650, https://doi.org/10.1016/j.heliyon.2020.e03650.
[7] C. Bombonnel, C. Vancaeyzeele, G. Guérin, F. Vidal, Fabrication of bicontinuous double networks as thermal and pH stimuli responsive drug carriers for on-demand release, Mater. Sci. Eng. C 109 (2020) 110495, https://doi.org/10.1016/j.msec.2019.110495.
[8] F. Fang, M. Li, J. Zhang, C.-S. Lee, Different strategies for organic nanoparticle preparation in biomedicine, ACS Mater. Lett. 2 (2020) 531–549, https://doi.org/10.1021/acsmaterialslett.0c00078.
[9] L. Pavoni, D.R. Perinelli, G. Bonacucina, M. Cespi, G.F. Palmieri, An overview of micro- and nanoemulsions as vehicles for essential oils: formulation, preparation and stability, Nanomater 10 (2020), https://doi.org/10.3390/nano10010135.
[10] Y. Dai, D. Yang, D. Yu, S. Xie, B. Wang, J. Bu, B. Shen, W. Feng, F. Li, Engineering of monodisperse core–shell up-conversion dendritic mesoporous silica nanocomposites with a tunable pore size, Nanoscale 12 (2020) 5075–5083, https://doi.org/10.1039/C9NR10813K.
[11] M. Gunaseelan, S. Yamini, G.A. Kumar, J. Senthilselvan, Highly efficient upconversion luminescence in hexagonal NaYF4:Yb3+, Er3+ nanocrystals synthesized by a novel reverse microemulsion method, Opt. Mater. 75 (2018) 174–186, https://doi.org/10.1016/j.optmat.2017.10.012.
[12] S.A. Tovstun, V.F. Razumov, Preparation of nanoparticles in reverse microemulsions, Adv. Chem. 80 (2011) 996–1012 (in Russian).
[13] T. Szumełda, A. Drelinkiewicz, R. Kosydar, J. Gurgul, D. Duraczyńska, Synthesis of carbon-supported bimetallic palladium–iridium catalysts by microemulsion: characterization and electrocatalytic properties, J. Mater. Sci. (2020), https://doi.org/10.1007/s10853-020-05277-z.
[14] K.R. Lange, Surfactants: Synthesis, Properties, Analysis, Application, Professiya, 2007 (in Russian).
[15] V.P. Mithila Boche, Microemulsion assisted transdermal delivery of a hydrophilic anti-osteoporotic drug: formulation, in vivo pharmacokinetic studies, in vitro cell osteogenic activity, J. Appl. Pharm. Sci. (2020) 8–19, http://japsonline.com/abstract.php?article_id=3187.
[16] M.S. Orellano, C. Porporatto, J.J. Silber, R.D. Falcone, N.M. Correa, AOT reverse micelles as versatile reaction media for chitosan nanoparticles synthesis, Carbohydr. Polym. 171 (2017) 85–93.
[17] X. Zhao, H. Zhu, J. Chen, Effects of sodium bis(2-ethylhexyl) sulfo succinate (AOT) reverse micelles on physicochemical properties of soy protein, Food Bioprod. Process. 94 (2015) 500–506, https://doi.org/10.1016/j.fbp.2014.07.009.
[18] Z. Li, R. Li, T. Mu, Y. Luan, Ionic liquid assisted synthesis of au–Pd bimetallic particles with enhanced electrocatalytic activity, Chem. Eur. J. 19 (2013) 6005–6013.
[19] M.G. Pineda, S. Torres, L.V. López, F.J. Enriquez-Medrano, R.D. De León, S. Fernández, H. Saade, R.G. López, Chitosan-coated magnetic nanoparticles prepared in one-step by precipitation in a high-aqueous phase content reverse microemulsion, Molecules 19 (2014) 9273–9287.
[20] L.M. Nikolenko, A.V. Ivanchihina, S.B. Brichkin, V.F. Razumov, Ternary AOT/water/hexane systems as "micellar sieves" for cyanine dye J-aggregates, J. Colloid Interface Sci. 332 (2009) 366–372, https://doi.org/10.1016/j.jcis.2008.12.022.
[21] G.M.S. Gomes, R.C.F. Bonomo, C.M. Veloso, L.H.M. da Silva, R.C.I. da Fontan, O.R.R. Gandolfi, G.R.F. Gonçalves, V.S. Sampaio, Acquisition of water solubility diagrams in ternary systems (AOT/organic solvent/alcohol) and extraction of $α$-lactalbumin using reverse micellar systems, J. Surfactant Deterg. 20 (2017) 831–841.
[22] S.S. Pawar, I. Regupathi, B.D. Prasanna, Reverse micellar partitioning of Bovine Serum Albumin with novel system, Resour. Technol. 3 (2017) 491–494, https://doi.org/10.1016/j.reffit.2017.06.004.
[23] M.P. Pileni, Structure and Reactivity in Reverse Micelles, Elsevier, Netherlands, 1989, http://inis.iaea.org/search/search.aspx?orig_q=RN:22006006.
[24] T. Kinugasa, A. Hisamatsu, K. Watanabe, H. Takeuchi, A reversed micellar system using mixed surfactants of sodium bis(2-ethylhexyl)sulfosuccinate and di(2-ethylhexyl)phosphoric acid for extraction of proteins, J. Chem. Eng. Jpn 27 (1994) 557–562, https://doi.org/10.1252/jcej.27.557.
[25] K. Shiomori, Y. Kawano, R. Kuboi, I. Komasawa, Extraction of proteins and water with sodium bis(2-ethylhexyl) sulfosuccinate/long chain alkyl amines mixed micellar system, J. Chem. Eng. Jpn 32 (1999) 177–183, https://doi.org/10.1252/jcej.32.177.
[26] B.S. Gupta, C.-R. Shen, M.-J. Lee, Effect of biological buffers on the colloidal behavior of sodium dodecyl sulfate (SDS), Colloids Surf. A Physicochem. Eng. Asp. 529 (2017) 64–72.
[27] A. Sadana, Protein refolding and inactivation during bioseparation, Sep. Sci. Technol, Elsevier 1998, pp. 287–312.
[28] S. Abbate, G. Longhi, A. Ruggirello, V.T. Liveri, Confinement of chiral molecules in reverse micelles: FT-IR, polarimetric and VCD investigation on the state of dimethyl tartrate in sodium bis(2-ethylhexyl) sulfosuccinate reverse micelles dispersed in carbon tetrachloride, Colloids Surf. A Physicochem. Eng. Asp. 327 (2008) 44–50, https://doi.org/10.1016/j.colsurfa.2008.06.001.
[29] S. Mandal, S. De, Copper nanoparticles in AOT "revisited"-direct micelles versus reverse micelles, Mater. Chem. Phys. 183 (2016) 410–421, https://doi.org/10.1016/j.matchemphys.2016.08.046.
[30] H. Kunieda, K. Shinoda, Solution behavior of aerosol ot/water/oil system, J. Colloid Interface Sci. 70 (1979) 577–583, https://doi.org/10.1016/0021-9797(79)90065-1.
[31] T. Kawai, K. Hamada, N. Shindo, K. Kon-no, Formation of AOT Reversed Micelles and W/O Microemulsions, Bull. Chem. Soc. Jpn. 65 (1992) 2715–2719, https://doi.org/10.1246/bcsj.65.2715.
[32] M. Kotlarchyk, J.S. Huang, S.H. Chen, Structure of AOT reversed micelles determined by small-angle neutron scattering, J. Phys. Chem. 89 (1985) 4382–4386, https://doi.org/10.1021/j100266a046.
[33] T. Hellweg, W. Eimer, The micro-structures formed by Ni2+-AOT/cyclohexane/water microemulsions: a light scattering study, Colloids Surf. A Physicochem. Eng. Asp. 136 (1998) 97–107, https://doi.org/10.1016/S0927-7757(97)00307-5.
[34] J. Eastoe, T.F. Towey, B.H. Robinson, J. Williams, R.K. Heenan, Structures of metal bis(2-ethylhexylsulfosuccinate) aggregates in cyclohexane, J. Phys. Chem. 97 (1993) 1459–1463, https://doi.org/10.1021/j100109a035.

[35] R.A. Day, B.H. Robinson, J.H.R. Clarke, J.V. Doherty, Characterisation of water-containing reversed micelles by viscosity and dynamic light scattering methods, J. Chem. Soc. Faraday Trans. 1 Phys. Chem. Condens. Phases 75 (1979) 132–139.

[36] A. Holmberg, L. Piculell, B. Wesslén, Viscosity effects of a graft copolymer with a hydrophobic backbone and hydrophilic side chains in a water/AOT/cyclohexane oil-continuous microemulsion, J. Phys. Chem. 100 (1996) 462–464, https://doi.org/10.1021/jp9527158.

[37] Y. Yoshimura, I. Abe, M. Ueda, K. Kajiwara, T. Hori, Z.A. Schelly, Apparent molar volume of solubilized water in AOT/isooctane/water reverse micellar aggregates, Langmuir 16 (2000) 3633–3635, https://doi.org/10.1021/la981209h.

[38] P.D. Moran, G.A. Bowmaker, R.P. Cooney, J.R. Bartlett, J.L. Woolfrey, Vibrational spectroscopic study of the structure of sodium bis(2-ethylhexyl)sulfosuccinate reverse micelles and water-in-oil microemulsions, Langmuir 11 (1995) 738–743, https://doi.org/10.1021/la00003a012.

[39] A. D'Aprano, A. Lizzio, V.T. Liveri, F. Aliotta, C. Vasi, P. Migliardo, Aggregation states of water in reversed AOT micelles: Raman evidence, J. Phys. Chem. 92 (1988) 4436–4439, https://doi.org/10.1021/j100326a038.

[40] M. Bey Temsamani, M. Maeck, I. El Hassani, H.D. Hurwitz, Fourier transform infrared investigation of water states in aerosol-ot reverse micelles as a function of counterionic nature, J. Phys. Chem. B 102 (1998) 3335–3340, https://doi.org/10.1021/jp971844g.

[41] D. Fioretto, M. Freda, S. Mannaioli, G. Onori, A. Santucci, Infrared and dielectric study of Ca(AOT)2 reverse micelles, J. Phys. Chem. B 103 (1999) 2631–2635, https://doi.org/10.1021/jp9837028.

[42] G. Onori, A. Santucci, IR investigations of water structure in Aerosol OT reverse micellar aggregates, J. Phys. Chem. 97 (1993) 5430–5434, https://doi.org/10.1021/j100122a040.

[43] G. Giammona, F. Goffredi, V. Turco Liveri, G. Vassallo, Water structure in water/AOT/n-heptane microemulsions by FT-IR spectroscopy, J. Colloid Interface Sci. 154 (1992) 411–415, https://doi.org/10.1016/0021-9797(92)90156-G.

[44] M. D'Angelo, G. Onori, A. Santucci, Structure of water-in-oil microemulsions of AOT by infrared spectroscopy, Nuovo Cim. D. 16 (1994) 1601–1611, https://doi.org/10.1007/BF02462048.

[45] P.D. Moran, G.A. Bowmaker, R.P. Cooney, J.R. Bartlett, J.L. Woolfrey, Vibrational spectra of metal salts of bis (2-ethylhexyl) sulfosuccinate (AOT), J. Mater. Chem. 5 (1995) 295–302.

[46] I.V. Plastinin, S.A. Burikov, S.P. Gofurov, O.B. Ismailova, Y.A. Mirgorod, T.A. Dolenko, Features of self-organization of sodium dodecyl sulfate in water-ethanol solutions: theory and vibrational spectroscopy, J. Mol. Liq. 298 (2020) 112053, https://doi.org/10.1016/j.molliq.2019.112053.

[47] A. Maitra, T.K. Jain, Study of the vibrational characteristics of aerosol OT by laser raman spectroscopy, Coll. Surf. 28 (1987) 19–27, https://doi.org/10.1016/0166-6622(87)80163-4.

[48] A.H. Khani, A.M. Rashidi, G. Kashi, Synthesis of tungsten nanoparticles by reverse micelle method, J. Mol. Liq. 241 (2017) 897–903, https://doi.org/10.1016/j.molliq.2017.06.053.

[49] G. Zhou, Z. Luo, X. Fu, Preparation and characterization of starch nanoparticles in ionic liquid-in-oil microemulsions system, Ind. Crop. Prod. 52 (2014) 105–110, https://doi.org/10.1016/j.indcrop.2013.10.019.

[50] J. Crain, W.C.K. Poon, A. Cairns-Smith, P.D. Hatton, High-pressure Raman spectroscopic study of cyclohexane C6H12 and C6D12, J. Phys. Chem. 96 (1992) 8168–8173, https://doi.org/10.1021/j100199a064.

[51] T.A. Dolenko, S.A. Burikov, S.A. Dolenko, A.O. Efitorov, I.V. Plastinin, V.I. Yuzhakov, S.V. Patsaeva, Raman spectroscopy of water-ethanol solutions: the estimation of hydrogen bonding energy and the appearance of clathrate-like structures in solutions, J. Phys. Chem. A 119 (2015), https://doi.org/10.1021/acs.jpca.5b06678.

[52] I.V. Plastinin, S.A. Burikov, T.A. Dolenko, Laser diagnostics of self-organization of amphiphiles in aqueous solutions on the example of sodium octanoate, J. Mol. Liq. 317 (2020) 113958, https://doi.org/10.1016/j.molliq.2020.113958.

[53] I.V. Plastinin, S.A. Burikov, S.A. Dolenko, T.A. Dolenko, Contribution of Fermi and Darling–Dennison resonances to the formation of Raman spectra of water and water–ethanol solutions, J. Raman Spectrosc. 48 (2017)https://doi.org/10.1002/jrs.5207.

[54] G.E. Walrafen, M.R. Fisher, M.S. Hokmabadi, W.-H. Yang, Temperature dependence of the low-and high-frequency Raman scattering from liquid water, J. Chem. Phys. 85 (1986) 6970–6982.

[55] S.A. Burikov, T.A. Dolenko, V.V. Fadeev, I.I. Vlasov, Revelation of ion hydration in Raman scattering spectral bands of water, Laser Phys. 17 (2007) 1255–1261.

[56] T.A. Gogolinskaya, S.V. Patsaeva, V.V. Fadeev, On the regularities of change of the 3100–3700 $см^{-1}$ band of water Raman scattering in salt aqueous solutions, Dokl. Akad. Nauk SSSR 1986, pp. 1099–1103.

[57] Sotiris S. Xantheas, Cooperativity and hydrogen bonding network in water clusters, Chem. Phys. 258 (2000) 225–231.

[58] Q. Sun, Local statistical interpretation for water structure, Chem. Phys. Lett. 568 (2013) 90–94.

[59] A.Y. Sdobnov, M.E. Darvin, J. Schleusener, J. Lademann, V.V. Tuchin, Hydrogen bound water profiles in the skin influenced by optical clearing molecular agents - quantitative analysis using confocal Raman microscopy, J. Biophotonics 12 (5) (2019) https://doi.org/10.1002/jbio.201800283.

[60] I.V. Plastinin, S.A. Burikov, T.A. Dolenko, S.A. Dolenko, Manifestation of Fermi resonance in Raman spectra of micellar aqueous solutions of sodium octanoate, Saratov Fall Meet. 2019 Laser Physics, Photonic Technol. Mol. Model 2020, p. 114580V, https://doi.org/10.1117/12.2560462.

[61] I.V. Plastinin, S.A. Burikov, S.A. Dolenko, T.A. Dolenko, The role of Fermi and Darling–Dennison resonances in the formation of the Raman spectra of water and water–ethanol solutions, Bull. Russ. Acad. Sci. Phys. 83 (2019)https://doi.org/10.3103/S1062873819030171.

[62] T.A. Dolenko, S.A. Burikov, S.A. Dolenko, A.O. Efitorov, Y.A. Mirgorod, Raman spectroscopy of micellization-induced liquid–liquid fluctuations in sodium dodecyl sulfate aqueous solutions, J. Mol. Liq. 204 (2015) 44–49, https://doi.org/10.1016/j.molliq.2015.01.021.

[63] M. Wong, J.K. Thomas, T. Nowak, Structure and state of water in reversed micelles. 3, J. Am. Chem. Soc. 99 (1977) 4730–4736, https://doi.org/10.1021/ja00456a034.